TÉCNICO LISBOA

In situ evaluation of the thermal performance of rammed earth walls

Extended abstract

Sofia Gama Caldas Sampaio

Thesis to obtain the Master of Science Degree in

Arquitecture

May 2014

ABSTRACT

Improve and modernize the earth construction is essential to spread its application. Despite of its high thermal inertia, the thermal resistance of the earth is usually not able to meet the requirements of thermal building regulations and that is one of the main obstacles in applying this technique.

In this study, the results of in situ measurement campaigns, carried out during the summer and winter periods, are presented. They were performed on three different single-family dwellings located in Abrantes, Portugal. These dwellings were built using the rammed-earth technique, each one having walls with 50-55 cm of thickness. Several experimental measurements were conducted in order to evaluate the rammed-earth wall thermal behavior, such as: the incident global radiation on vertical plane of the facade; indoor and outdoor environment temperatures and moisture; indoor and outdoor surfaces wall temperatures; and heat fluxes. Moreover, walls' thermal conductivity, volumetric heat capacity and thermal diffusivity were also obtained using a portable measuring instrument.

The experimental results revealed a large thermal inertia of the walls, which led to low indoor temperatures in both seasons. The results also demonstrate the need to improve the thermal conductivity of the earth in order to meet the requirements of the building regulations.

Keywords: *rammed-earth walls, in situ measurement, thermal conductivity*

NOTATION

λ – Thermal conductivity (W/m.ºC)

α – Thermal diffusivity (m^2/s)

$c\rho$ – Volumetric heat capacity ($J/m^3.K$)

U – Heat transfer coefficient ($W/m^2.ºC$)

R_{si} – Indoor thermal resistance ($m^2.ºC/W$)

R_{se} – Outdoor thermal resistance ($m^2.ºC/W$)

e – wall thickness (m)

1. INTRODUCTION

The earth construction is known for their large walls and their pleasant indoor temperatures during very warm summers which explain the use of this material in hot climates. In Portugal there is a vast heritage, particularly in Alentejo and in the interior of Portugal, where the maximum temperatures in summer can, generally, rise above 40ºC. As a benefit of the large thickness, the earth's walls have a high thermal inertia which is responsible for the delay of the heat conduction throughout the walls, contributing for mild inside temperatures. Also, their large mass can accumulate the heat inside the walls and, consequently, it can reduce the use of heating energy once they can function as a heat source [1]. However, the thermal resistance value of earth walls is usually very low and this represents a problem when facing the building regulations [2, 3, 4, 5].

Although the large experience in living in earth's constructions since the remote ages, the concepts of sustainable construction and thermal comfort are relatively new and the scientific documentation of earth's construction thermal behaviour and improvement solutions, so it can be used as a modern material, is still scarce.

This paper presents the results of two in situ measurement campaigns during two different periods, summer and winter, carried out in three dwellings located in the region of Abrantes, Portugal. There were monitoring the vertical global radiation, the indoor and outdoor environment temperatures and moisture; indoor and outdoor surfaces wall temperatures; and heat flows. The performance of the earth walls is examined by analysing the evolution of the indoor and outdoor heat flow through the walls and the indoor and outdoor temperatures with the influence of the incident solar radiation. Furthermore, the thermal conductivity, the volumetric heat capacity and the thermal diffusivity of the earth walls are also determinate in situ.

2. EXPERIMENTAL WORK

Two different experimental tests were carried out in order to characterize the thermal behaviour of earth's construction case studies. The first test aims to analyse the inside temperature evolution according to the outdoor temperature and incident radiation. In order to have a general perception of the thermal behaviour, two campaigns were held in extreme Portuguese climate situations: one during the winter period and another during the summer period. From each campaign the extreme day – so on called as Day Type - was chosen and analysed. These Days Type represent the coldest and the warmest day during winter and summer campaign, respectively, for CS1 and CS2. The second test intends to measure the thermal conductivity, volumetric heat capacity and thermal diffusivity of a representative portion of the wall using a portable measuring instrument.

The case studies are located in the region of Abrantes, N39°27'52"; W8°11'52", Portugal, which characteristically has dry and very warm summers and mild and wet winters. Table 1 presents the monitoring periods of each case study.

Table 1. Monitoring periods of each case study

		CS1	CS2	CS3
Winter	Start	4th February, 12h20	12th February, 15h00	8 de Março, 14h10
	End	12th February, 10h30	8th March, 11h20	28 de Março, 12h00
	Duration	7 days, 22 hours and 10 min.	23 days, 20 hours and 20 min.	19 dias, 21 horas e 50 min.
Summer	Start	25th May, 12h30	15th June, 14h40	*N.A
	End	15th June, 15h30	4th July, 13h00	*N.A
	Duration	21 days and 3 hours	18 days, 22 hours and 20 min.	*N.A

* N.A - Not applicable. The CS3 was unavailable during summer campaign so the campaign was not realized.

The outdoor temperatures and the incident global radiation on vertical plane during both the winter and summer campaigns for the two case studies are summarized in Table 2.

Table 2. Maximum, minimum and average outdoor temperatures and radiation of both case studies during the two campaigns (winter and summer) in CS1 – case study 1, CS2 – case study 2 and CS3 – case study 3.

		CS1		CS2		CS3
		Winter	Summer	Winter	Summer	Winter
Temperature (ºC)	Max	23,37	32,30	19,23	41,66	18,61
	Min	0,37	8,72	-0,65	12,52	1,81
	Mean	10,00	16,76	9,96	23,08	11,23
Radiation (W/m^2)	Max	1033,53	570,80	889,03	829,34	757,46
	Min	0	0	0	0	0
	Mean	188,55	32,70	97,07	91,36	96,46

The dwellings are uninhabited and have doors and windows closed. During the campaign, 2 thermocouples Type T were used to measure surface wall temperatures (T_{se} and T_{si}); PTC sensor for environment temperatures (T_e and T_i); and 2 heat flow meters installed on the indoor and outdoor wall surfaces, to measure de heat flow. It was also installed one thermo-hygrometer (Rotronic HydroLog-D) to measure the indoor relative humidity and temperature. For the outdoor temperature, it was used data from the weather station of Abrantes (courtesy of Hélder Silvano Neves – MeteoAbrantes). Finally, a pyranometer LICOR 200 was installed on the façade to measure the incident global radiation on vertical plane.

A data logger NCE 2520-00 Network Control Engine by Metasys®, with remote transmission, was programmed to take measurements with intervals of 1 in 1 minute and record the average of these values each 10 minutes.

In order to measure the thermal conductivity, thermal diffusivity and volumetric heat capacity of the earth wall the portable measuring instrument ISOMET 2114 was used, as described in session 4.

3. CASE STUDIES

The case study 1 is located in Casais de Revelhos, Abrantes, Portugal. The main façade was the monitored one and is facing south, which has 55 cm thick. There are no shade elements so the probes are exposed directly to the solar radiation. Due to the poor conservation along the 100 years of existence, some house components, such as the ceiling and doors are very damage, so the airtightness is not completely assured.

Figures 1 and 2 show, respectively, a photograph of the dwelling's façade and a sketch of the probes location.

Figure 1. Monitored façade (south façade)

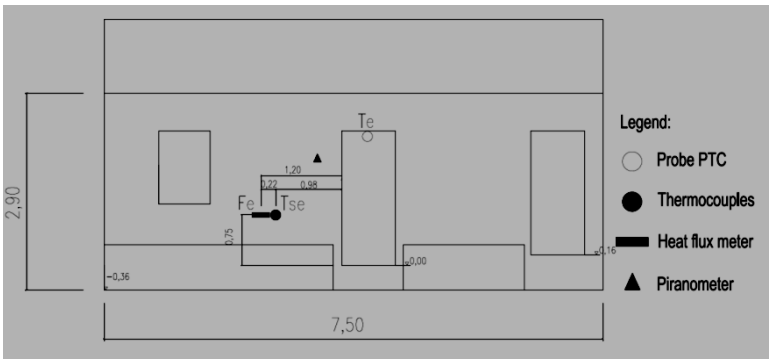

Figure 2. South façade's sketch with probes' location

The case study 2 is located in Pego, Abrantes, Portugal. The main facade is facing north; the monitored façade was the one facing west and the walls have 50 cm of thickness. Nevertheless, the PTC sensor for the outdoor temperature measurement was installed near the window of the north façade so that the solar radiation does not influence the values.

Although it is not recommended to install the equipment near a thermal bridge, in this case it was not possible to avoid the location of some probes near the corner between the north and the west walls because of the length of the probes' cables.

Figures 3 and 4 show a photograph of the dwelling's north and west façades and Figure 5 shows a sketch of the probes location.

Figure 3. North façade

Figure 4. Monitored façade (west façade)

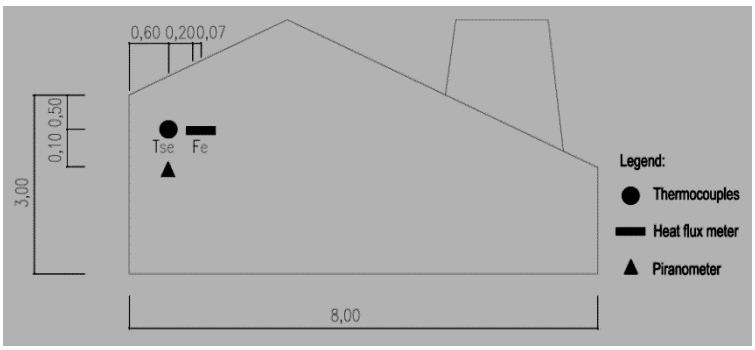

Figure 5. Sketch of the west façade with probes' location

Case study 3 is also located in Pego, Abrantes, Portugal. The main facade was the monitored one and is facing south. There are also no shade elements. Unfortunately, due to some unforeseen contingencies, it was not possible to carry out the summer campaign in this case study.

Figure 6. Monitored façade (South façade).

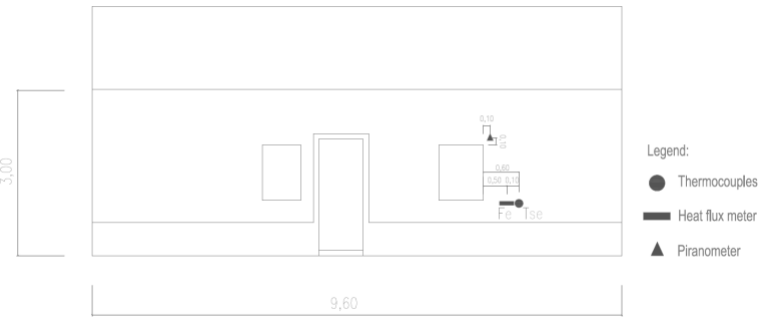

Figure 7. Sketch of the south façade with probes' location.

4. TEMPERATURE AND HEAT FLUX ANALYSIS

The results were organized by campaign and only the results of the extreme days will be presented, in particularly the coldest and the warmest day for winter and summer, respectively, for each dwelling.

4.1 Winter Campaign

During the winter campaign one façade of each dwelling was monitored (see Chapter 2). The data recorded and the results of the monitoring coldest day in winter campaign are presented in Figures 6 and 7.

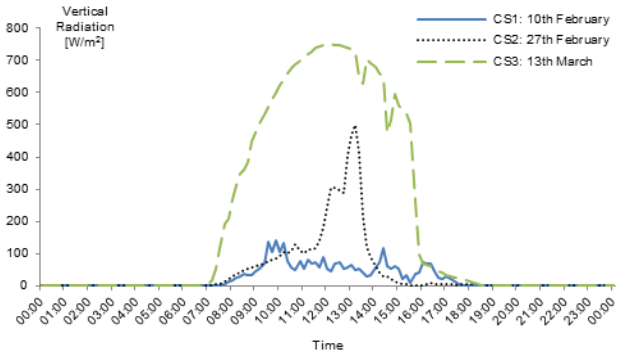

Figure 8. Incident global radiation on the vertical plane of the façades in the coldest winter monitoring day.

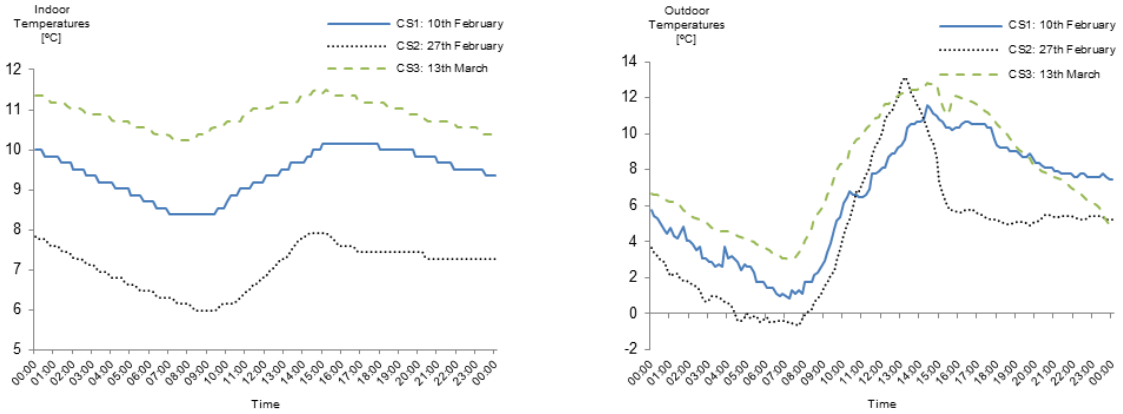

a. **b.**

Figure 9. Temperatures in the coldest winter monitoring day: a. Indoor environment ; b. Outdoor environment

Figure 8 and 9 show that the dwellings were exposed to similar outdoor temperatures values (Figure 9.b), even when the incident solar radiation (Figure 8) on the monitored façade plane shows very high values, such as in CS3. The maximum outdoor temperature was between 12 ºC and 14 ºC and the minimum was between -1 ºC and 3 ºC. Also, the indoor temperatures were quite similar and compared to the outdoor temperatures had very small temperature variation (Figure 9.a). The outdoor temperature amplitude was about 14 ºC, whereas the indoor temperature amplitude was less than 2 ºC.

Figure 8 also shows that the maximum value of solar radiation in CS2 was registered later, during the afternoon, as expected, because the monitored façade is west oriented. The other cases, CS1 and CS3, are south oriented.

Figure 10 presents the indoor and outdoor heat flow with the influence of the solar radiation and the horizontal profil of temperatures at different hours of the day. Heat flows are assumed as positive when taking the outdoor-indoor direction. In Figure 10 (a., c. and e.) it is possible to notice that the outdoor heat flow was highly influenced by the incident solar radiation, whereas the indoor heat flow was generally close to zero. Moreover, Figure 10 (a., c. and e.) shows that the indoor heat flow had, during daytime, an opposite signal to

the outdoor heat flow. Therefore, the heat flow, in most cases, did not have just one way, which means that the wall was accumulating heat during the daytime. As a result, the indoor temperature was relatively stable along the day in both case studies, although the outdoor temperature decreased a lot during the night. Despite that, the indoor temperature was always considerably below the comfort indoor temperatures for winter period (18 ºC [8]).

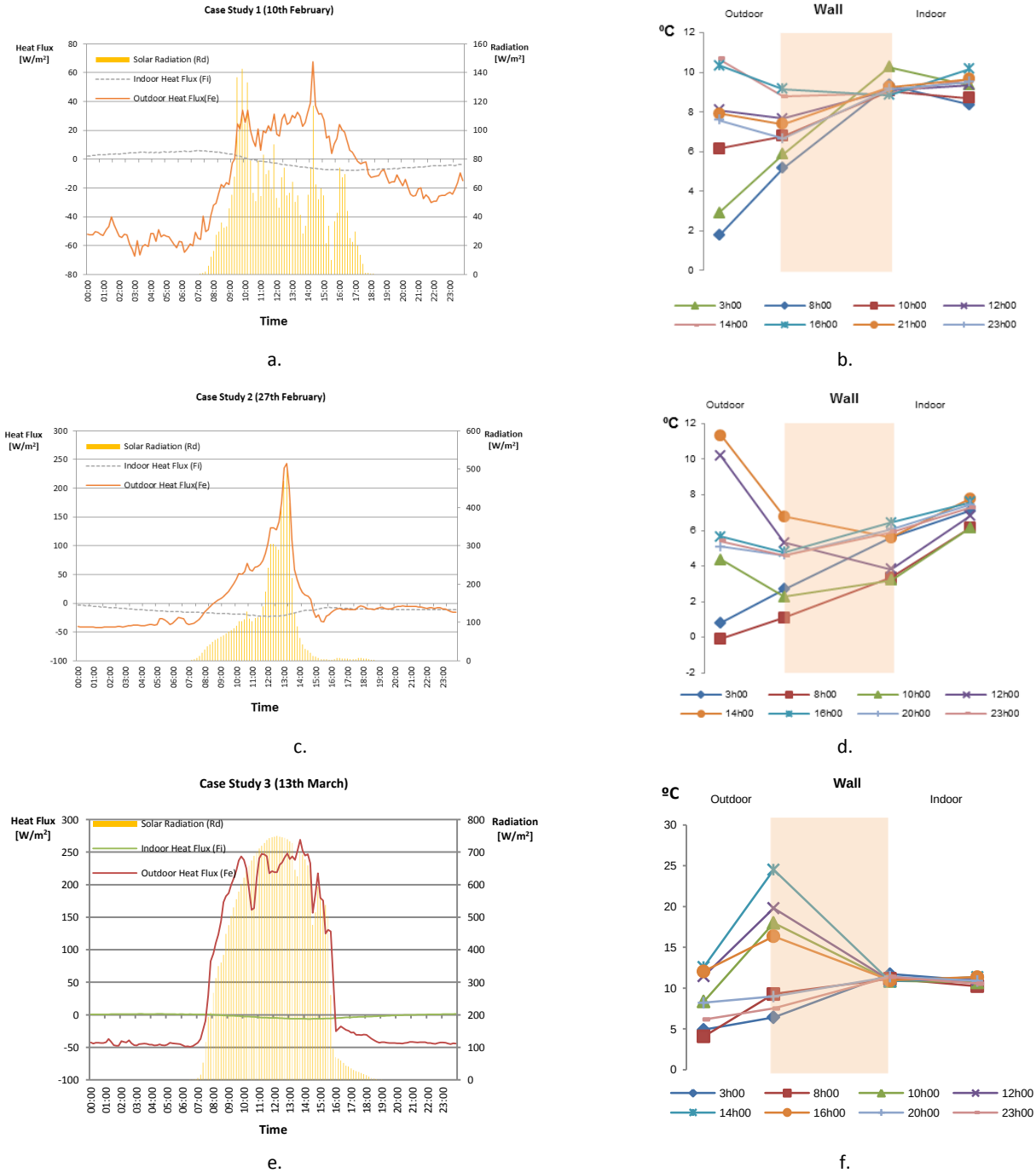

Figure 10. Incident global radiation on the vertical plane of the façade and heat flow and heat flow through the wall (a., c. and e.); horizontal profiles of temperature (b., d. and f.) in the coldest winter monitoring day for CS1, CS2 and CS3.

4.2 Summer Campaign

The results of indoor and outdoor temperatures and incident global radiation on vertical plane during the summer campaign of the warmest monitoring day are presented in Figure 11 and 12.

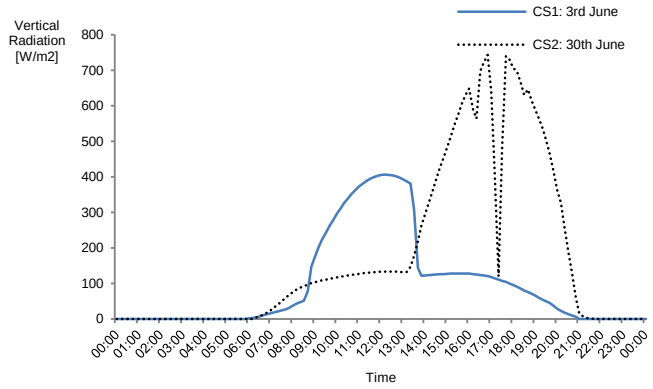

Figure 11. Incident radiation on the vertical plane of the façades in the warmest summer monitoring day.

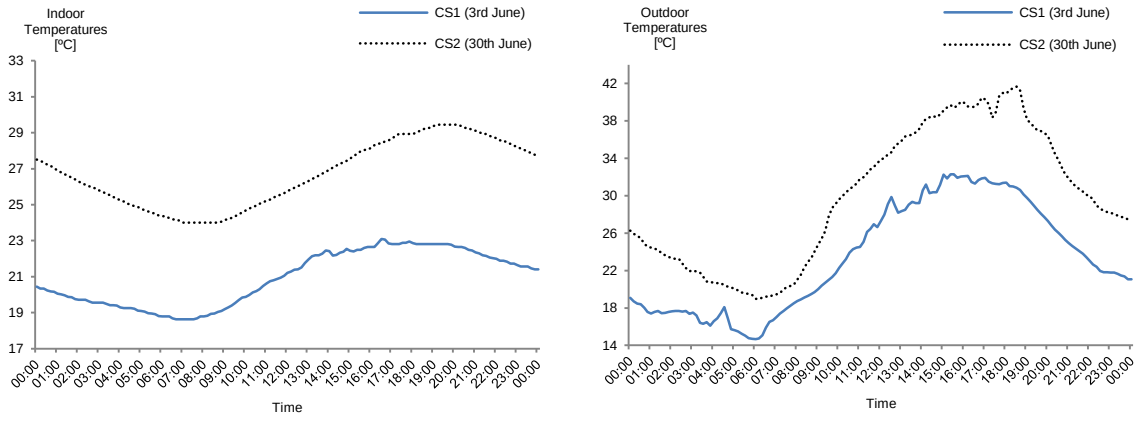

a. b.

Figure 12. Temperatures in the warmest summer monitoring day; a. Indoor environment; b. Outdoor environment

In the summer campaign the recorded data shows conformity between the outdoor temperatures conditions and the solar radiation. By Figure 12 it is possible to observe that CS2 was exposed to very high temperatures during all day and a high solar radiation incidence (Figure 11). As referred before, the monitored façade in CS2 was west oriented, which explains the highest values during the afternoon. Figure 11 shows that the solar radiation in CS1 had a big drop in the middle of the daylight that could be explained by a cloudy afternoon.

In this campaign, the maximum outdoor temperature (Figure 12.b.) was around 30 ºC (in CS1) and 42 ºC (in CS2) and the minimum was around 14 ºC (in CS1) and 20 ºC (in CS2). This means that the outdoor temperature amplitude reached 22 ºC in CS2. Once again, the indoor temperatures were quite similar in both case studies and in comparison to the outdoor temperatures they showed a very small temperature variation.

Figure 13 a. and c. shows very high values of the outdoor heat flows (with outdoor-indoor direction) clearly influenced by solar radiation, where the maximum values of the heat flow coincide with the maximum value of the incident solar radiation. As in the winter campaign, the indoor heat flow was almost null, which indicated that the solar radiation was absorbed and the heat accumulated in the walls during the daytime.

The indoor heat flow, in most of the cases, had an opposite signal to the outdoor heat flow. When the outdoor heat flow reached its highest value, the indoor heat flow reached its lowest value. Almost at the same

time, it was registered the highest value for the indoor environment. As it is represented in Figure 13.b., despite the indoor surface temperature almost did not vary, the indoor temperature registered higher variation. As so, it is possible to conclude that the variation of the indoor temperature is mostly due to the heat conduction throw the ceiling, door and windows and not throw the earth walls. For case study 2, Figure 13.d., the same effect happened from 8h00 to 14h00, however around 16h00 (Figure 13. c. and d.) the heat flux became positive and reached the highest values. This means that thermal inertia in CS2 is lower than in CS1 because the delay between the highest value of outdoor and indoor heat flux is superior in CS1.

Also, Figure 13.d. shows that the indoor surface temperature variation in CS2 was higher than in CS1 which demonstrates a lower thermal inertia of CS2 wall.

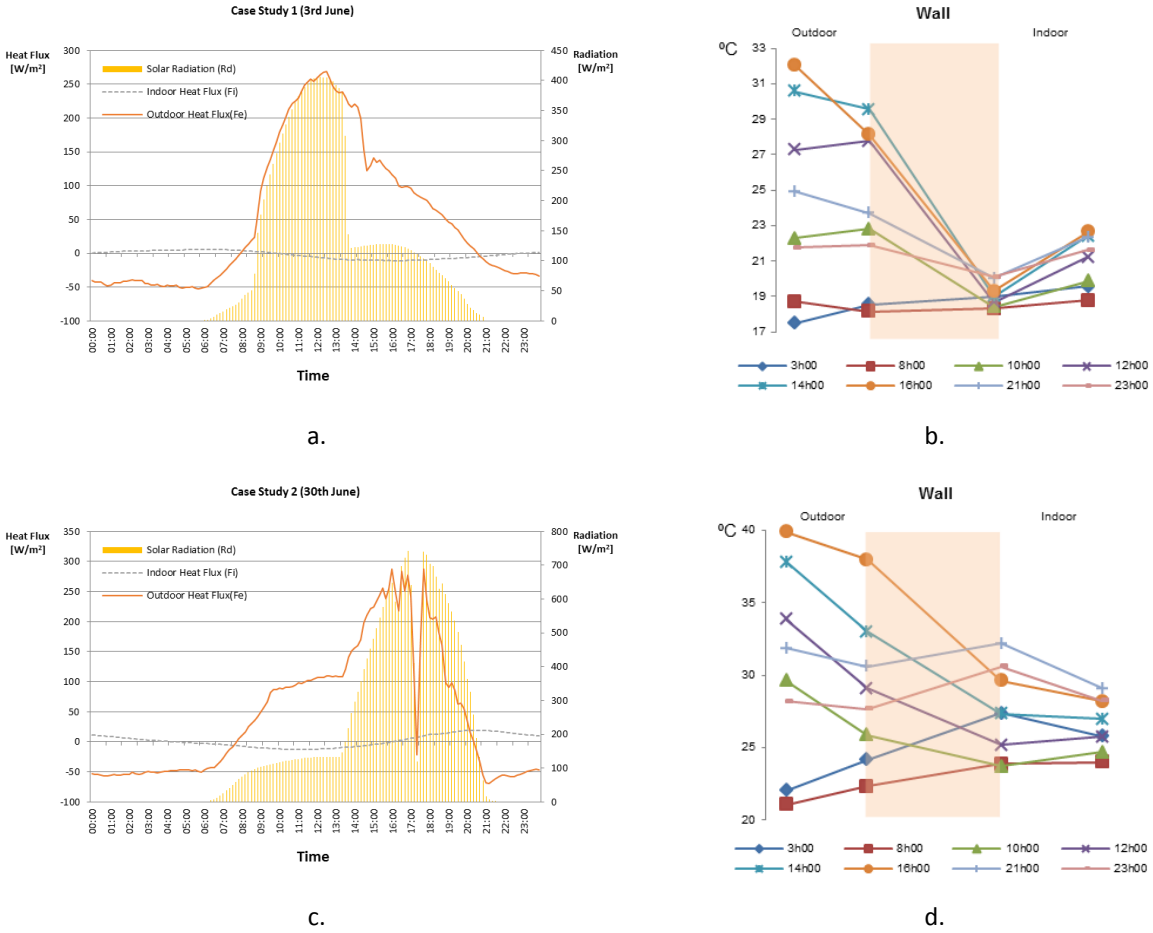

Figure 13. Incident global radiation on the vertical plane of the façade and heat flow and heat flow through the wall (a. and c.); horizontal profil of temperature (b. and d.) in the warmest summer monitoring day for CS1 and CS2.

The outdoor heat flow has positive signal while is registered values of the solar radiation. Without its incidence, the outdoor heat flow could be near zero as well the indoor heat flow. Observing Figure 13.c., heat flow and solar radiation variation graphic for CS2, one can see that there was a moment, around 17h30, where the solar radiation crushed abruptly and, as a consequence, the outdoor heat flow reached a negative value.

Concerning the temperatures distribution (Figure 13 b. and d.), it is possible to observe higher temperature variation for the outdoor parameters (outdoor temperature and outdoor surface temperature).

There is a considered delay between the outdoor and the indoor temperatures maximum values. At 16h00 it was registered the highest outdoor temperature for CS2, whereas the highest indoor environment temperature was only reached at 21h00. This is a result of the high thermal inertia of the earth constructions.

In general, the summer monitoring campaign results are coherent with the ones obtained during the winter campaign.

5. THERMAL CONDUCTIVITY AND DIFFUSIVITY ANALYSIS

As it was previously explained, this second analysis intends to determine both thermal conductivity and thermal diffusivity values of the earth walls from each case study. While thermal conductivity (λ) is the property of a material to conduct heat, thermal diffusivity measures the ability of a material to conduct thermal energy relative to its ability to store thermal energy. In fact thermal diffusivity (α) is the thermal conductivity (λ) divided by density and specific heat capacity at constant pressure [7].

The equipment used to perform this test was the ISOMET 2114, from Applied Precision enterprise, which is a portable hand-held measuring instrument for direct measurement of heat transfer properties of a wide range of isotropic materials including cellular insulating materials, plastics, glasses and minerals. It is equipped with two optional types of measurement probes: needle probes for soft materials; surface probes for hard materials. A dynamic measurement method is applied, which enables to reduce the measurement time in comparison with the steady state measurement methods [6]. This equipment allows, by the imposition of a thermal pulse, the measurement of the thermal conductivity, λ, in a range between 0.015 and 0.70 W/m.K, with a maximum error of 5% ±0.001 W/m.K and between 0.70 to 6.0 W /m.K with a maximum error of 10%; and the thermal diffusivity, α by calculating the volumetric heat capacity (cρ) in a range of 4,0 $x10^4$-4,0 $x10^6$ $J/m^3.K$ with an accuracy of 15 % of reading + $1,10^3$ $J/m^3.K$.

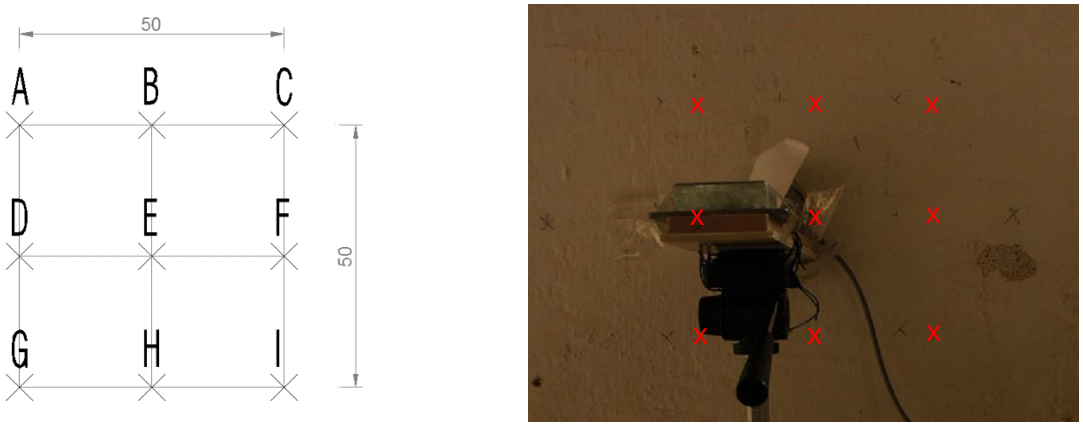

a. b.

Figure 14. a. Representative measurement points in the wall; b. Test in progress in case study 1.

To perform the test, it is recommended to measure thermal conductivity in several points in a representative portion of the wall, due to the heterogeneity of rammed earth walls. Therefore, in a square of 50 cm side, 9 points were measured in order to have a larger sample of values (Figure 14). Thereafter, the thermal conductivity of the earth walls was obtained by calculating their mean value.

It is important to point out that the test was carried out during winter and the humidity content of the walls' surface was high which can strongly influence the results.

5.1 Results and discussion

Table 3 presents thermal conductivity, volumetric heat capacity and thermal diffusivity mean values for both case studies.

Observing Table 3 it is possible to verify that the average values for thermal conductivity are 0,74 W/m.ºC for CS1, 0,98 W/m.ºC for CS2 and 0,85 W/m.ºC for CS3. Thermal diffusivity (α), in turn, registered for CS1 a

value of 0,51 m^2/s, 0,64 m^2/s for CS2, and, finally of 0,61 m^2/s for CS3. These values lead us to a better thermal behavior of CS1 earth wall.

On the other hand, the standard deviation of thermal conductivity results demonstrate that rammed earth walls in CS1 are more heterogeneous. The standard deviation is 0,26 W/m.ºC for CS1, 0,17 W/m.ºC for CS2 and 0,20 W/m.ºC for CS3.

By Table 3. it is possible to verify that CS2 has poorer thermal characteristics. Even if the volumetric heat capacity is higher, thermal conductivity is too high and, as a result, the thermal diffusivity of the earth wall of CS2 is higher than CS1 and CS3.

Table 3. Mean and standard deviation values of thermal conductivity, thermal diffusivity and volumetric heat capacity of both case studies.

	λ (W/m.ºC)		cρ (J/m^3.K) x10^6		α (m^2/s) x10^6	
	Mean value	Standard deviation	Mean value	Standard deviation	Mean value	Standard deviation
CS1	0,74	0,26	1,44	0,04	0,51	0,17
CS2	0,98	0,17	1,48	0,08	0,64	0,15
CS3	0,85	0,20	1,41	0,04	0,61	0,13

Figure 15 shows the survey of the wall using the measured values of λ , cρ and α in each point, of the three case studies (CS1, CS2 and CS3). CS3 shows greater uniformity of λ values, a part of point I, in which the value is much higher.

CS1, in turn, has greater variability. The points located in the upper left corner recorded higher values while lower values were registered in the lower right corner. It is also the CS1 case study that shows lower values (predominantly situated in green scale), particularly the H and I area. CS2 registered higher values than the other case studies (predominantly yellow scale).

Regarding volumetric specific heat (cρ) survey, it shows great uniformity in all case studies (red tone).

Since the thermal diffusivity results by the division between the thermal conductivity (W/m.ºC) and the volumetric specific heat (cρ), once cρ remains uniform, it is expected that the thermal diffusivity survey (Figure 15.c) seems similar to the thermal conductivity survey (Figure 15.a.).

After determining thermal conductivity values it is possible to calculate the heat transfer coefficient (U-value) for the studied earth walls by equation 1

$$U = \frac{1}{R_{si} + R_{se} + \frac{e}{\lambda}} \ (\text{W/m}^2.\text{ºC}) \quad (1)$$

Where:

U – Heat transfer coefficient (W/m^2.ºC)

R_{si} – Indoor thermal resistance (m^2.ºC/W)

R_{se} – Outdoor thermal resistance (m^2.ºC/W)

e – wall thickness (m)

λ – Thermal conductivity (W/m.ºC)

As described before, the earth wall thickness was 0,55 m in CS1 and 0,50 m in CS2. Adopting indoor and outdoor surface thermal resistance (R_{si} and R_{se}) of 0,13 m^2.ºC/W and 0,04 m^2.ºC/W, respectively [8], the U-values are 1,09 W/m^2.ºC for CS1 and 1,47 W/m^2.ºC for CS2.

For external wall in Abrantes (I2 zone) the maximum value allowed for heat transfer coefficient is 1,60 W/m^2.ºC which means that both case studies meet the regulation. However, taking into account the reference value for I2, that is 0,40 W/m^2.ºC and from 2016 will be 0,35 W/m^2.ºC, the U-values obtained are too high and very unsatisfactory.

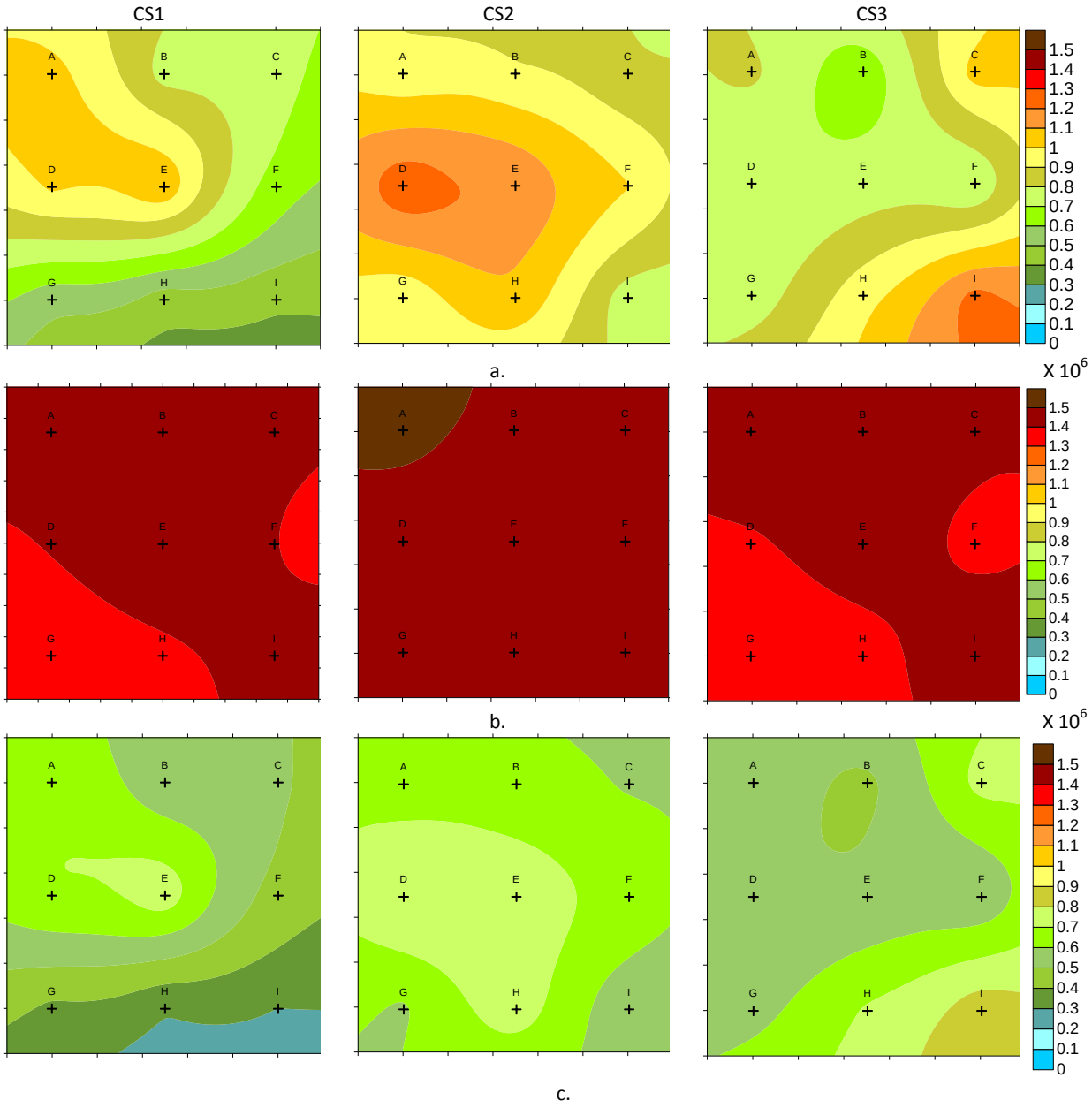

Figure 15. a.Thermal conductivity survey; b. volumetric heat capacity survey; c. thermal diffusivity survey.

6. CONCLUSIONS

This study aimed to characterize the thermal behavior of earth constructions by in situ experimental tests. For that, indoor and outdoor temperatures, relative humidity, heat fluxes and incident radiation were registered for both summer and winter periods in uninhabited dwellings in Abrantes, Portugal. Also thermal conductivity was measured with a portable measuring equipment.

The following conclusions can be drawn from the present study:

- The indoor thermal comfort of the earth's constructions is not achieved during the winter extreme conditions.
- However, during summer extreme conditions its behavior is very satisfactory.
- The temperatures difference between indoor and outdoor environments is very high due to the high thermal inertia of the earth walls.
- Although the high outdoor temperature variation (almost 22 ºC in CS2 during summer campaign) the indoor temperature variation in very small.
- The outdoor heat flow is highly influenced by the incident solar radiation.
- The opposite signals for the outdoor and indoor heat flows during the daytime indicate that the solar radiation is being absorbed by the wall and the heat is accumulated. This is enhanced by the high thermal inertia of the wall.
- There is a considered delay between the outdoor and the indoor temperatures maximum values which is also due to the high thermal inertia of the wall.
- The experimental results revealed a large thermal inertia of the walls, which led to low indoor temperatures in both seasons.
- Average thermal conductivity values were 0,74 W/m.ºC for CS1 and 0,98 W/m.ºC for CS2.
- CS1 shows better average thermal conductivity and lower values for thermal diffusivity than CS2.
- Standard deviation of thermal conductivity and diffusivity values in CS1 are higher than in CS2 which means that CS1 wall is more heterogeneous.
- The heat transfer coefficient is 1,09 W/m^2.ºC and 1,47 W/m^2.ºC for CS1 and CS2 respectively.
- The results demonstrate the need to improve the thermal conductivity (λ) and the heat transfer coefficient (U-value) of the earth in order to meet the recommended values from the thermal building regulations (0,40 W/m^2.ºC).

REFERENCES

[1] Ip, K., Miller, A., (2009), Thermal behaviour of an earth-sheltered autonomous building – The Brighton Earthship, Renewable Energy 34, Issue 9, pp. 2037-2043.

[2] Clarke, R (2010) Thermal Resistance of Rammed Earth Walls - CSIRO Press Release, CSIRO.

[3] Goodhew, S., Griffiths, R., Short, D. and Watson, L., (2000); Some preliminary studies of the thermal properties of Devon cob walls, Terra 2000, 8th International Conference on the Study and Conservation of Earthen Architecture, pp. 139-143.

[4] Goodhew, S., Griffiths, R., (2005); Sustainable earth walls to meet the building regulations, Energy and Buildings 37, Issue 5, pp. 451-459.

[5] Hall, M.R., (2005) Assessing the environmental performance of stabilized rammed earth walls using a climatic simulation chamber, Building and Environment 42, Issue 1, pp. 139-145.

[6] Isomet product catalog – English (ISOMET-PC201104-EN) (2011), Applied Precision Ltd (http://www.appliedp.com/download/catalog/isomet_pc_en.pdf).

[7] Kittel, C.; Kroemer, H. (1980). *Thermal Physics*. W. H. Freeman and Company. Chapter 14. ISBN 978-0716710882.

[8] DL118/2013 de 20 de Agosto, Regulamento de desempenho energético dos edifícios de habitação (REH), 2013.